1

Thermal Effects in Optical Fibres

Paulo André, Ana Rocha, Fátima Domingues and Margarida Facão
Instituto de Telecomunicações and Departamento de Física, Universidade de Aveiro Portugal

1. Introduction

Optical fibres are essential components in the modern telecommunication scenario. From the first works dealing with the optimization of optical fibres transmission characteristics to accommodate long distance data transmission, realized by Charles Kao (Nobel Prize of Physics in 2009), until the actual optical fibre communication networks, a long way was paved.

The developments introduced in the optical communication systems have been focused in 3 main objectives: increase of the propagation distance, increase of the transmission capacity (bitrate) and reduction of the deployment and operation costs. The achievement of these objectives was only possible due to several technological breakthroughs, such as the development of optical amplifiers and the introduction of wavelength multiplexing techniques. However, the consequence of those developments was the increase of the total optical power propagating along the fibres.

Moreover, in the last years, the evolution of the optical networks has been toward the objective of deploying the fibre link end directly to the subscribers home (FTTH – fibre to the home).

Thus, the conjugation of high power propagation and tight bending, resulting from the actual FTTH infrastructures, is responsible for fibre lifetime reduction, mainly caused by the local increase of the coating temperature. This effect can lead to the rupture of the fibre or to the fibre fuse effect ignition with the consequent destruction of the optical fibre along kilometres.

In this work, we analyze the thermal effects occurring in optical fibres, such as the coating heating due to high power propagation in bent fibres and the fibre fuse effect. We describe the actual state of the art of these phenomena and our contribution to the subject, which consists on both experimental and numerical simulation results.

2. Literature review

The fibre fuse effect, named due to the similarity with a burning fuse, was first observed in 1987 (Kashyap, 1987; Kashyap et al., 1988). At that time, the effect was observed on a single mode silica fibre illuminated by an optical signal with an average power density higher than $5MW/cm^2$. Like a burning fuse, after the optical fibre fuse ignition, the fuse zone propagates towards the light source while a visible white light is emitted. After the fuse zone propagation, the fibre core shows a string of voids, being permanently damaged. The phenomenon was always associated with a thermal effect and although there are not yet very accurate experimental data for the actual temperature achieved in the fibre core, it is believe that the peak temperature is up above the silica vaporization point, around 3300 K. Some authors also refer that the white light emission characteristic of this effect may indicate temperatures that would allow plasma like fuse zone (10^4) (Hand et al., 1988[b;] Dianov et al., 2006; Shuto, 2010).

The first explanation for the effect related it to a thermal self-focusing mechanism (Kashyap et al., 1988). Afterwards, the fuse zone was identified as a soliton-like thermal shock-wave which would occur by strong thermal dependent absorption due to the creation of Ge-related defects in Ge doped core fibre. To sustain this hypothesis, the a Ge doped fibre was heated up to 1000ºC in the absence of any propagating optical signal and the same kind of periodic damaged pattern was produced (Driscoll et al., 1991), however this result has not been reproduced by any others research groups.

At the time of these first observations the fuse effect did not represent a practical problem, since the total power injected in the network optical fibres was well below the power densities used in the experiments. However, the rise of optical communications demand and the consequent increase of the injected power have promoted the fuse effect to one of the fundamental issues which should be considered while developing and maintaining optical networks. Hence, for several years the phenomenon was referred as the origin of the optical fibres damage, but only in the presence of high powers. It was only a few years ago that the scientific community turned to this effect in order to explain it better but also to design devices able to detect and halt this catastrophic effect.

Nowadays, the most accepted explanation for the fuse effect describes it as an absorption enhanced temperature rise that propagates toward the light source by thermal conduction and driven by the optical power itself. The first numerical simulation of the fuse propagation used an explicit finite-difference method where it was assumed that the electrical conductivity and consequently the absorption of the core increase rapidly above a given temperature, *Tc*. Using this thermally induced optical absorption, Tc of 1100 ºC and an optical power of 1 W, the core temperature was shown to reach 100000 ºC (Shuto et al., 2003), which is well above the temperature of the fuse zone measured by (Dianov et al., 2006).

Also, the trigger to ignite this effect was studied. The trigger is a high loss local point in the fibre network, usually in damaged or dirty connectors or in tight fibre bends that, combined with high power signals, generate a heating point (Andre et al., 2010[b]; Seo et al., 2003; Martins et al., 2009; Andre et al., 2010[a]). The specific mechanism associated with the fuse effect generation in optical connectors was also studied and correlated with the absorption of the dust particles in the connector end face (Shuto et al., 2004[c]).

Another important issue is the power density threshold to initiate and maintain the fibre fuse propagation. The investigation so far indicates that the power density threshold is ~1-5 MW/cm^2, depending on the type of fibre and on the signal wavelength (Davis et al., 1997; Seo et al., 2003). Note that the first experiments using microstructured fibres have shown that the optical power density threshold value to ignite the phenomena is 10 times higher in these fibres than in traditional step index silica fibres (Dianov et al., 2004[b]).

The increase of absorption that is believed to take place during fuse propagation was related with Ge' defects, as mentioned above, but also with Si E' defects in the Germanium doped silica core optical fibres. These defects are induced at high temperatures, like the temperatures present in the fibre drawing process (Hanafusa et al., 1985). The E' defects are associated with oxygen vacancies ≡Ge–Si≡ and are stable at temperatures above 870 K. The conjugation of this temperature dependent absorption mechanism with the absorption of the SiO specimen, produced by the thermal decomposition reaction of the Silica glass at high temperatures, occurring for temperatures above 3000 ºC, was considered by Shuto et al to numerically simulate the fuse effect ignition and propagation. He reported estimate for the Silica absorption coefficient was 10^7 m^{-1} at 6000 K for a wavelength of 1064 nm (Shuto, 2010).

Dianov et al has experimentally demonstrated that the radiation spectrum for the optical discharge, propagating through the silica fibre, is close to that of the blackbody with plasma temperature values of 10^{4} K. The observed optical discharge velocities were up to 10 m/s on step index single mode fibre (Dianov et al., 2006) and 30 m/s for Erbium doped fibre(Davis et al., 1997).

Atkins et al propose a model for the bubble and voids tracks based on the Rayleigh instability due to the capillary effects in the molten silica that surrounds the vaporised fibre core(Atkins et al., 2003). The void formation and other dynamics of the fibre fuse propagation were exhaustively studied, leading to models for the voids and bubbles shape (Todoroki, 2005[b;] Todoroki, 2005[c;] Yakovlenko, 2006[a]), and profile models for the optical discharge (Todoroki, 2005[a]). Todoroki has also shown that is possible to have optical discharge without the formation of voids, along short distances, being this responsible by the irregular patterns on the voids trail (Todoroki, 2005[d]).

Other authors have also observed and studied the fibre fuse effect in special fibres like hole assisted fibre (Hanzawa et al., 2010), high numerical aperture fibres (Wang et al., 2008), polarization maintaining fibres(Lee et al., 2006) or in dispersion shift and non zero dispersion shift fibres (Rocha et al., 2010; Andre et al., 2010[a]).

Recently, more accurate simulation models for fuse propagation have been proposed (Yakovlenko, 2006[b]), or even alternative models based on ordinary differential equations that represent time saving in the numerical integration (Facao et al., 2011).

The concern with the effects for the network structure caused by the triggering of the fuse effect imposes the development of devices with the capacity to stop the fuse zone propagation. An early solution proposed in 1989 was the use of single mode tapers (Hand et al., 1989). The decrease of the fibre cladding led to expansion of the optical discharge plasma and to decrease of the power density, this results in the termination of the fuse propagation (Dianov et al., 2004[a]). Others proposed solutions to detect the fuse effect that are based in the analysis of the electric spectrum of the back reflected optical signal (Abedin et al., 2009), or in the fast temperature increase in the fibre outer surface (Rocha et al., 2011).

The deployment of FTTH networks imposes a new challenge, the dissemination of the optical fibre infrastructure in the access networks, where the fibre installation conditions are not always the more adequate. In these conditions, the deployed fibre is subject to tight bending, which impose an additional attenuation for the network power budget. The additional attenuation of waveguides subject to tight bending is a well know phenomenon, studied in 1976 by Marcuse(Marcuse, 1976). Marcuse associated the additional losses in bent waveguides with the optical signal radiated to the cladding region, this model was later improved by other authors (Harris et al., 1986; Valiente et al., 1989; Schermer et al., 2007).

Besides the new attenuation limits imposed by the bending, other constrain was observed. For high propagation power signals, the optical modes irradiated to the cladding, are absorbed in the primary coating, resulting in a temperature increase. This local heating

point can induce the fuse effect already referred above or can reduce the fibre lifetime (Percival et al., 2000; Glaesemann et al., 2006; Sikora et al., 2007).
The first works on this subject have shown that the temperature achieved by the fibre coating was linearly correlated to the propagated optical power (Logunov et al., 2003). However, this linear model fails to describe the coating temperature for high power propagation (> 1 W), and recently an improved model that considers a nonlinear absorption coefficient for the coating was proposed (Andre et al., 2010[b]).
This topic has attracted the focus of the scientific community and many new achievements have been reported in the last years technical conferences. Namely, the correlation of temperature and fibre time failure (Davis et al., 2005), the definition of the safety bending limits (Andre et al., 2009; Rocha et al., 2009[a]). Recently, this topic was also studied in the new bend insensitive fibres (G.657), showing that the maximum power that can be injected safely in these fibres without coating risk is > 3 W (Bigot-Astruc et al., 2008).

3. Fibre fuse effect

As described in the previous section, the fibre fuse effect is a phenomenon that can occur in optical fibres in the presence of high optical powers and that may lead to the destruction of the optical fibre, along several kilometres, and also reach the optical emitter equipment, resulting in a permanent damage of the network active components.
However, the presence of high optical powers is not enough to ignite the fibre fuse but a trigger consisting of a initial heating point is also required. During the fuse effect ignition, this initial heating point causes a strong light absorption, due to the thermal induced absorption increase, which in turn leads to a catastrophic temperature increase, up to values that are high enough to vaporize the optical fibre core. This fuse zone propagates towards the light source melting and vaporizing the fibre core while a visible white light is emitted, as schematically illustrated in Fig 1. The propagation of the fuse zone only stops if the input power is reduced below the threshold value or even shut down. After the fuse zone propagation, the fibre core shows a string of voids, being permanently damaged.

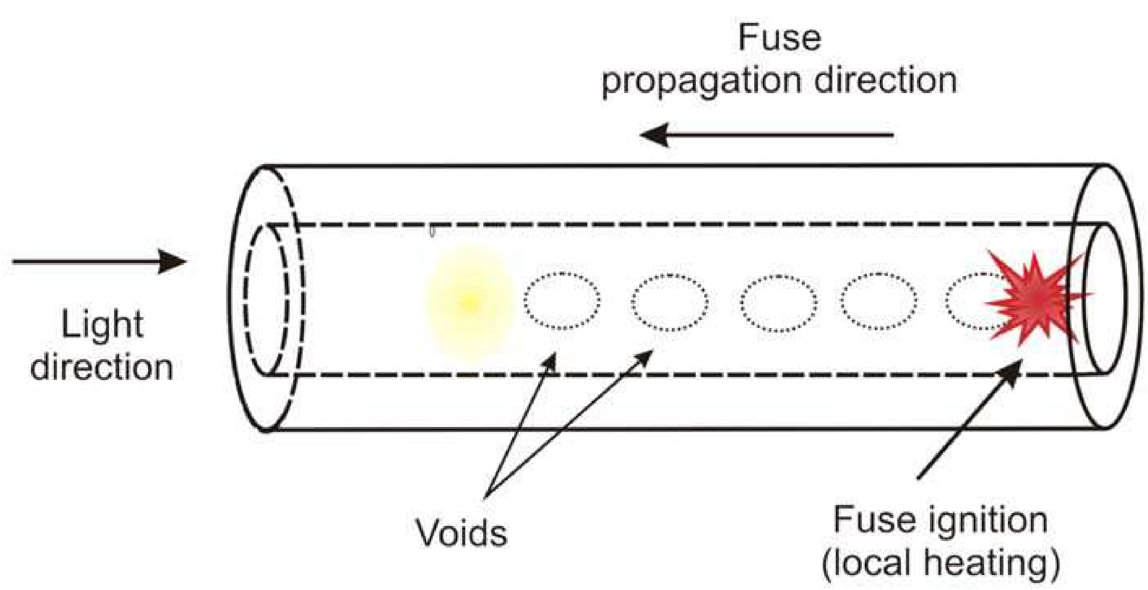

Fig. 1. Schematic representation of the fuse effect ignition and propagation in an optical fibre

3.1 Experimental characterization of the fuse effect

As referred above, the fibre fuse effect is initiated in a local heating point, whenever the optical signal have powers above a certain threshold value. Fig. 2 presents a controllable experimental setup for the fibre fuse ignition.

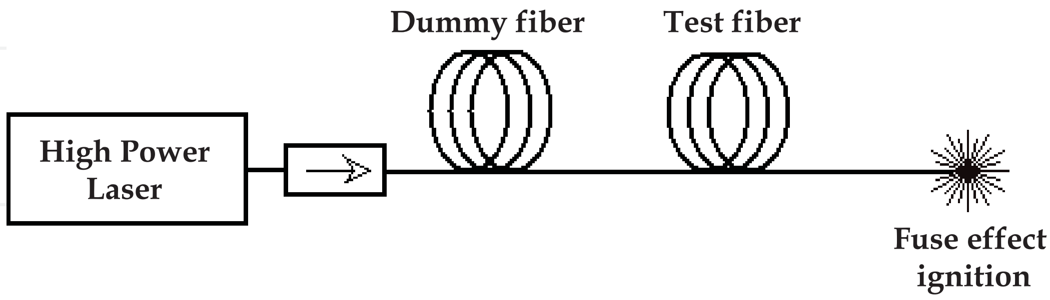

Fig. 2. Experimental setup implemented to study the fibre fuse effect (Rocha et al., 2011)

This setup consists in a short length of fibre (~3m) connected to a high power laser. The other end of the fibre is placed in contact with a metallic foil in order to produce a local heating and promote the fuse effect ignition. In order to protect the optical source, an optical isolator and a dummy fibre with 20 m are used between the test fibre and the laser.

Fig. 3 shows three frames from a movie, displaying the fuse propagation. In this movie, the white light emitted (optical discharge) from the fuse zone is clearly seen. The fuse discharge propagates at constant velocity towards the light source.

Fig. 3. Sequence of frames of the fibre fuse propagation in a SMF fibre, the time difference between pictures is 0.1s

As mentioned above, if the optical power is reduced below a threshold value, the fuse propagation stops and the optical discharge extinguishes. For standard single mode fibre (SMF-28, manufactured by Corning) and a laser signal with a wavelength of 1480 nm, the optical discharge extinguishes for an optical power of 1.39 W.

The fibre fuse propagation velocity increases with the optical power density, and could reach values high as 10 m/s (Dianov et al., 2006; Rocha et al., 2011). Fig. 4 presents the experimental velocities for the fuse effect propagation, ignited with a laser signal at 1480 nm in a SMF-28 fibre. These experimental results indicate that, for this limited range of optical power values, the fibre fuse propagation velocity is linearly dependent on the optical power launched into the fibre, however, if we consider higher optical power values, the velocity will be no longer a linear function function of the optical power (Dianov et al., 2006; Facao et al., 2011).

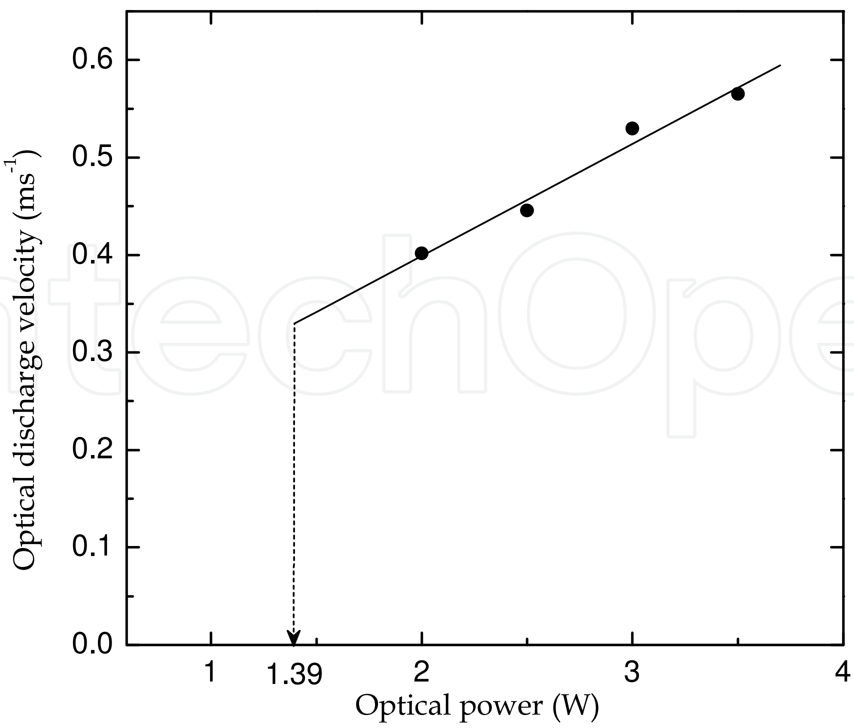

Fig. 4. Fuse discharge velocity as function of the injected optical power. The arrow represents the power threshold and the line correspond to the data linear fit (slope=0.110±0.002 m s^{-1} W^{-1}, intercept= 0.190±0.004 m s^{-1}, correlation coefficient > 0.993)

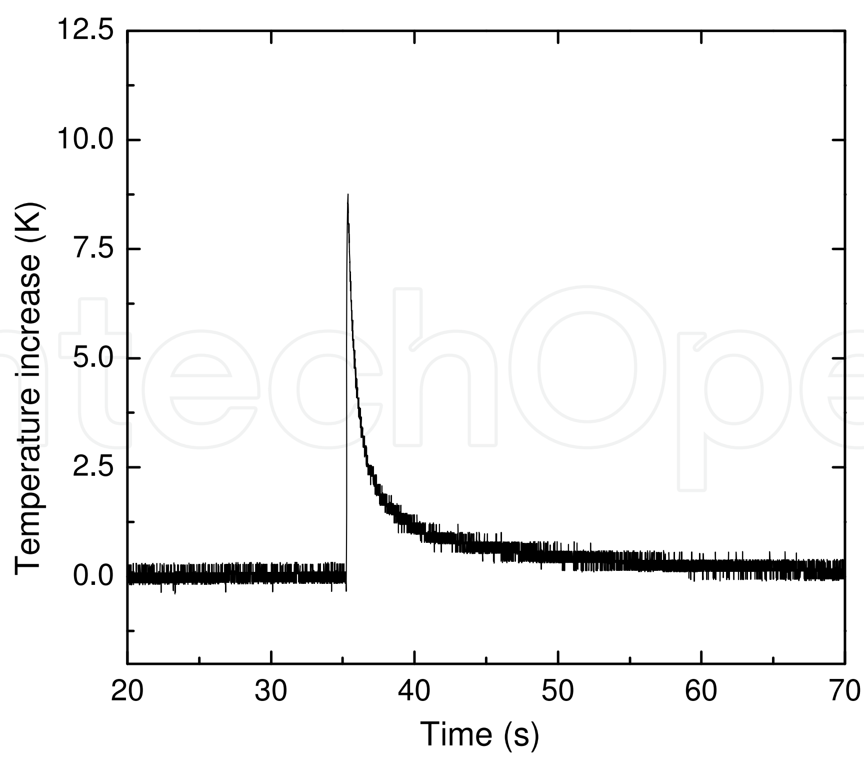

Fig. 5. Fibre surface temperature increase as a function of time, recorded by the FBG sensor during the optical discharge for an optical power of 3 W

The propagation velocity of the fuse zone was measured using a setup based on FBG (Fibre Bragg Grating) temperature sensors that measure the fibre outer interface temperature (Andre et al., 2010[a;] Rocha et al., 2011). Two fibres Bragg gratings were placed in contact with the optical fibre outer interface, in two positions separated by 2 m.

The optical discharge leads to a temperature increase in the outer fibre surface, which is monitored by the FBG sensors. The time difference between the temperature peaks, recorded at each FBG, is then used to obtain the velocity of the optical discharge. Fig. 5 displays the temperature increase in the fibre surface measured by one FBG. This graph presents an abrupt temperature increase, followed by an exponential decrease. The temperature peak corresponds to the optical discharge passing through the FBG location. Although, the fiber core is believed to achieve temperatures around 10^4 K during the optical discharge, the fiber surface temperature increases just a few degrees above the environmental temperature, as results of the heat transfer mechanisms (conduction, radiation and convection) that dissipate the thermal energy along the optical fiber and to the surrounding environment.

After the optical discharge propagation, the fibre presents a chain of voids in the core region that can be observed with an optical microscope. Fig 6 displays the optical microscopic images of the SMF fibre, obtained after the optical discharge propagation.

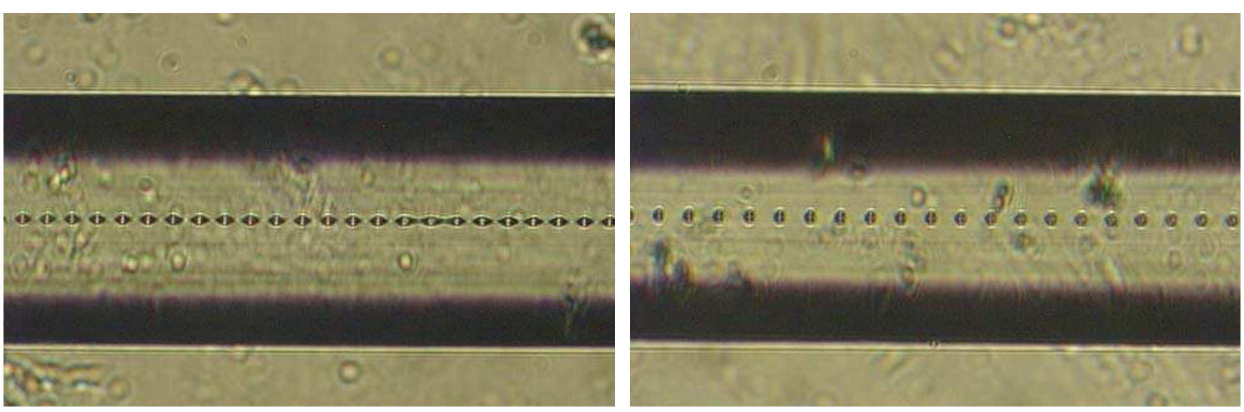

Fig. 6. Microscopic images of the optical fibre after the optical discharge propagation for optical powers of 2.5 W (right) and 4.0 W (left) (pictures obtained using an optical magnification of ×50)

These pictures were taken after the removal of the fibre coating. In these pictures, the damage caused by the fuse is clearly visible, the voids are created in the melted/vaporized core region with a periodic spatial distribution. The size and the spatial interval of the voids vary with the input power and the type of fibre (Andre et al., 2010[a]). Fig 7 shows the relation between the void period and the optical signal power. For this limited range of optical powers, the void period is linearly dependent on the optical power level.

3.2 Theoretical model

Even though many underlining phenomena that sustain the fuse effect are still not understood, the general explanation says that the initial high temperature zone, that ignite the effect, increases strongly the light absorption that, in turn, is responsible for the increase of the fibre temperature around 10^4 K (Dianov et al., 2006) well above the silica vaporization temperature. The localized high temperature zone spreads to neighbouring regions, due to heat conduction, and propagates into the laser direction, where the optical power signal is present to drive the spike up of the temperature. The process repeats causing the propagation of the optical discharge.

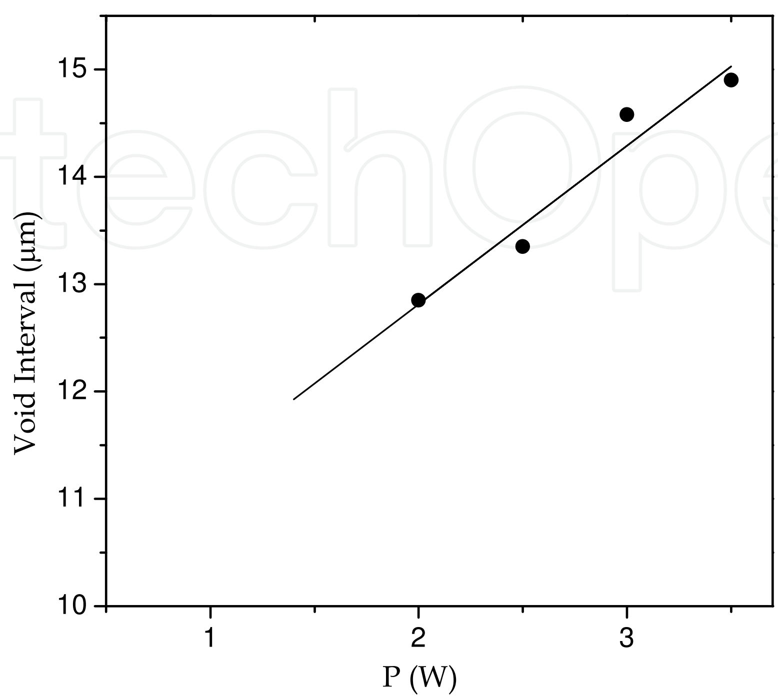

Fig. 7. Void period as function of the injected optical power at 1480 nm in a SMF-28 fibre. Points are experimental data and the line corresponds to the data linear fit (slope=1.38±0.06 µm W^{-1}, intercept=10.1±0.2 µm, correlation coefficient > 0.944)

To summarise, we assume that the main process taking place in the fibre during the fuse effect is a positive feedback heating process induced by temperature enhanced light absorption.

In the recent years, there has been substantial interest in the development of theoretical models for the fibre fuse phenomenon. Several hypotheses have been put forward to explain the strong absorption, but as we mentioned previously a lot of mechanisms are still to be understood, especially because it has been hard to measure the optical absorption at such high temperatures or even to chemically analyse the contents of the voids and their surrounding on a fuse damaged fibre. Nevertheless, most of these works propose a propagation model based on a heat conduction equation with a heat source term that corresponds to the optical signal absorption which itself is enhanced by the temperature rise. This equation is coupled to an ordinary differential equation (ODE) for the spatial evolution of the optical signal power (Shuto et al., 2003; Shuto et al., 2004[a;] Facao et al., 2011). Hence, let us model the fuse effect by a one-space-dimensional heat conduction equation coupled to an equation for the optical power evolution along the fibre length, namely:

$$
\begin{aligned}
&\rho c_p \frac{\partial T}{\partial t} = k \frac{\partial^2 T}{\partial z^2} + \frac{\alpha P}{\pi R^2} - \frac{2\sigma_s \varepsilon}{R}(T^4 - T_r^4), \\
&\frac{dP}{dz} = -\alpha P,
\end{aligned}
\tag{1}
$$

where $T(t,z)$ is the fibre temperature, P is the optical power, t is time and z is the longitudinal coordinate along the fibre distance, ρ, C_p and k are the density, the specific heat, and the thermal conductivity of the fibre, respectively and R is the optical signal mode field radius.
The second term of the heat conduction equation is the heat source, caused by light absorption, where $\alpha(T)$ is the local absorption coefficient and the last term represents the loss by radiation which is written in terms of the Stefan-Boltzmann constant, σ_s, the surface emissivity, ε, and the environment temperature, T_r.
The increase of the optical signal absorption coefficient, α, with temperature plays the most important role in the generation of the fibre fuse. It was reported that the absorption coefficient is temperature dependent and rapidly increases above a critical temperature (1000 ºC), moreover it achieves a very large value for temperatures above 2000ºC (Hand et al., 1988[a;] Hand et al., 1988[b;] Shuto et al., 2004[b]). In 1988, Hand and Russell suggested that the absorption increase is closely related with Ge defects that are supposedly created in the core of the fiber once the temperature rises. In their model the absorption dependence with temperature is described by an Arrhenius law (Hand et al., 1988[a]). Shuto *et al* (Shuto et al., 2004[b]) have also proposed that the formation of Ge related defects could increase the number of free electrons and the subsequent electrical conductivity of the fibre core then enhances the absorption. In their opinion, this mechanism would explain the absorption values reported by Kashyap (Kashyap et al., 1997). This latter model also results in an Arrhenius law. But since the fuse effect also occurs in fibres without germanium, other models of absorption increase that do not rely on the presence of germanium should be put forward. One of them, also proposed by *Shuto et al* (Shuto et al., 2004[b]) relates the absorption increase with the thermochemically formation of SiO at higher temperatures, this model would allow absorption values as large as 10^4 m^{-1} for 2293 K. They also propose that, for lower temperatures, the Ge-defects should be the main absorption mechanism but for higher temperatures the presence of SiO should be more relevant. Moreover, an Arrhenius law was also proposed to model this absorption of SiO. Therefore, even if more than one process promotes the temperature rise in fibers, whether they are doped with germanium or not, the experimental data that have been collected up to now seem to manifest that all of them are thermally induced, so they are the kind of processes that are frequently modeled by an Arrhenius law.
For the reasons presented above and since here we are mainly concerned with common fibres used in telecommunications, with Ge doped cores, we use the following Arrhenius law, proposed by Hand and Russell, to model the temperature dependent optical absorption coefficient (Hand et al., 1988[a]).

$$\alpha = \alpha_0 \exp\left(-\frac{E_f}{k_b T}\right) \tag{2}$$

where E_f = 2.5 eV (Shuto et al., 2004[a]) is the formation energy of the Ge defects, k_B is Boltzmann's constant and α_0 is a constant dependent on the light wavelength and on the optical fibre type.
As already stated, the fibre fuse phenomenon is initiated only in a local heating point, thus in our model we assume an initial hot zone with the temperature above the critical value T_c.

3.2.1 Simulation of the fibre fuse effect for a single mode fibre (SMF)

The system of equations (1) and (2) was integrated using a numerical routine from the NAG toolbox, *d03pp*, that integrates nonlinear parabolic differential equations with automatic adaptive spatial remeshing.

In this calculation it was assumed an optical signal source at 1480 nm, a mode field radius of 5.025 μm, that is the mode field radius for the optical fibre used in the experimental characterization (SMF-28) at this wavelength and the same thermal proprieties of the silica glass, since the Ge concentration is very low. In this study the variation of the thermal proprieties and energy loss during changes of phase or even chemical reactions that should occur for such high temperatures were neglected, therefore, we have used the constant thermal coefficients of the silica glass listed in table 1. The equations were solved for a 3 cm long fiber with a initial hot zone of 0.2 mm centered within the fiber, and considering T_c=2900K and an environment temperature of 300 K.

ρ	2200 kg m^{-1}
k	2 Wm^{-1}K^{-1}
C_p	1430 JKg^{-1}K^{-1}

Table 1. Thermal coefficients of silica glass (Sergeev et al., 1982; Facao et al., 2011)

Since the absorption dependence with temperature is not exactly known and, particularly, the parameter of the Arrhenius law here proposed were not yet determined for this wavelength neither for such high temperatures, the parameter α_0 was adjusted with the model described in (Facao et al., 2011) which gave $\alpha_0 = 4.56\times10^6$ m^{-1}.

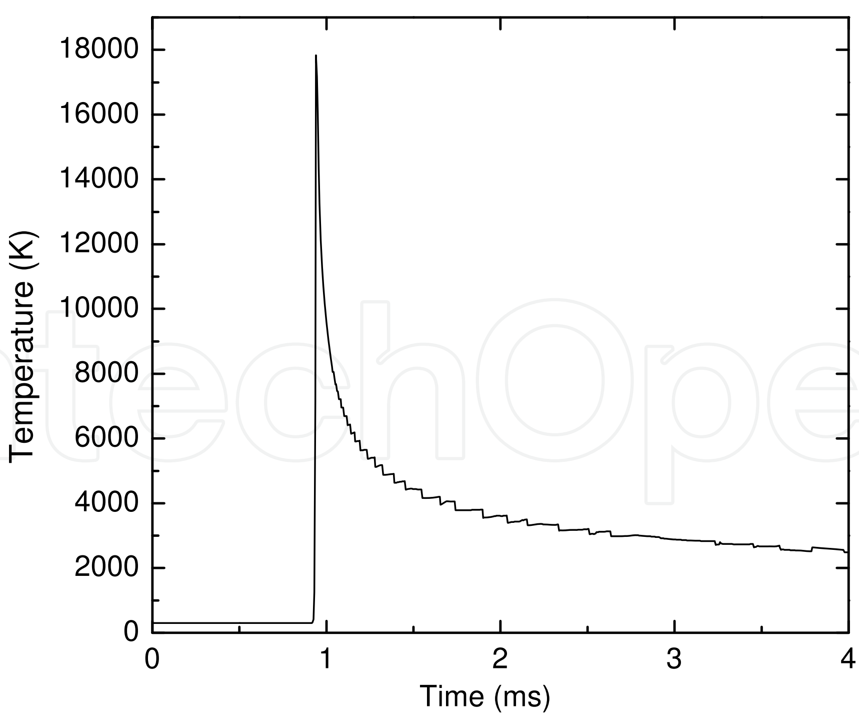

Fig. 8. Fibre core temperature at a fixed point as function of time for an optical power of 3 W

Fig. 8 displays the temperature peak that corresponds to the hot zone passing through a fixed point in the fiber. It shows an abrupt change in temperature followed by an exponential decrease. This temperature pulse is similar to the one obtained in the experimental characterization but achieves a much higher temperature. Recall that, in the experimental characterization, the measured temperature was done in the outer surface of the fiber and the temperature obtained numerically is estimated in the fiber core. Then, the temperature pulses moves in the negative-z direction (direction of the light source) with constant velocity (see Fig 9 (a)).

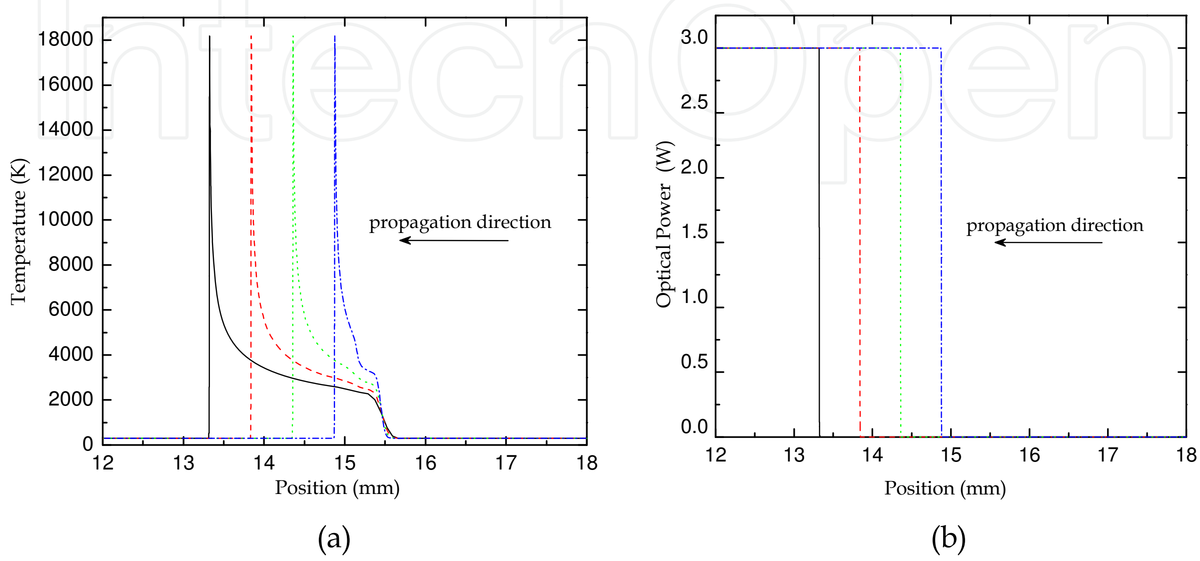

Fig. 9. Temperature (a) and power (b) distribution profiles along the propagation axis at several temporal moments spaced by 1 ms, for an optical power of 3W (the profile timing increases from the right to the left)

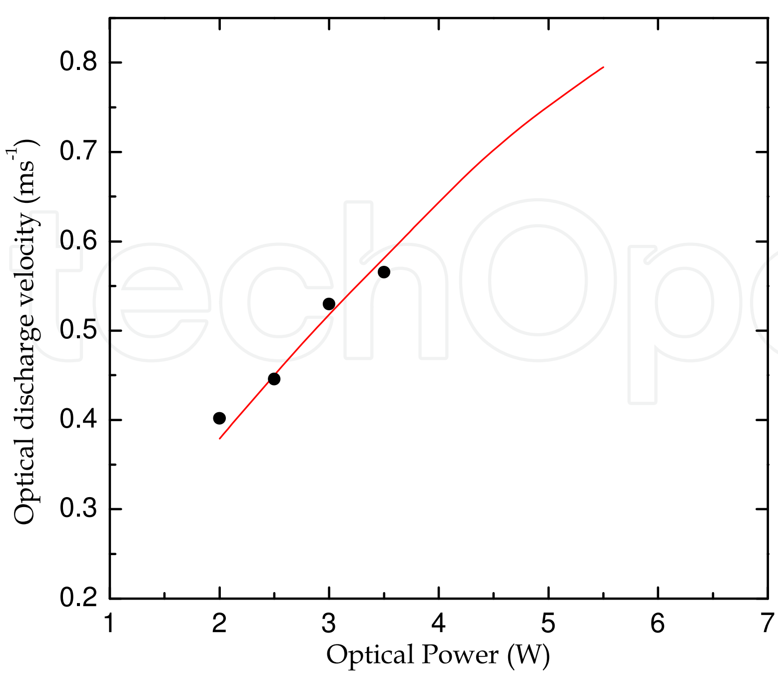

Fig. 10. Experimental (points) and numerical values (line) for the optical discharge propagation velocity as function of the injected optical power

Fig. 9 shows the travelling pulses of the optical discharge and the travelling fronts of optical power in several temporal moments. In the fuse zone all the incident optical signal is absorbed, scattered or reflected and the transmitted optical power decreases abruptly down to a null value.

The velocities obtained in this calculation are compared with the experimental values in Fig. 10, showing a good agreement with a relative error smaller than 6%.

As mentioned in section 3.2, for a limited range of relatively low optical power values, the fiber fuse propagation velocity is linearly dependent on the optical power, yet Fig 10 shows that the relation of the velocity with power density is not linear if a wider range is considered.

4. Optical fiber coating temperature increase

The increase of the temperature in an optical fibre is one of the responsible causes for its degradation. This increase in the temperature can be due to the high optical powers propagating in regions with small bending diameters. In these regions, part of the optical signal transfers from the core of the fibre to the surrounding cladding and coating (Bigot-Astruc et al., 2006; Giraldi et al., 2009; Rocha et al., 2009[a]; Rocha et al., 2009[b]). This effect can lead to the degradation of the protection layers of the fibre, with the consequent rupture, or even to the fibre fuse effect ignition.

Some recent works have studied the optical fiber resistance to high optical power (Logunov et al., 2003). The maximum attained temperature value has been studied, based on a thermal model for low power propagation signals (<1W) (Percival et al., 2000).

Here, we report our study about coating temperatures of an optical fiber, when subjected to low bending and high power optical signals. The coating temperature and the optical power loss were measured for different bend diameters. For that purpose, we have implemented an experimental setup consisting in a circular loop whose radius is controllable, as sketched and imaged in Fig. 11. The setup was designed in order to assure that the fiber suffer a bend of 360º without any change of radius. The bend diameters under study comprised values between 2.95 mm and 20.14 mm.

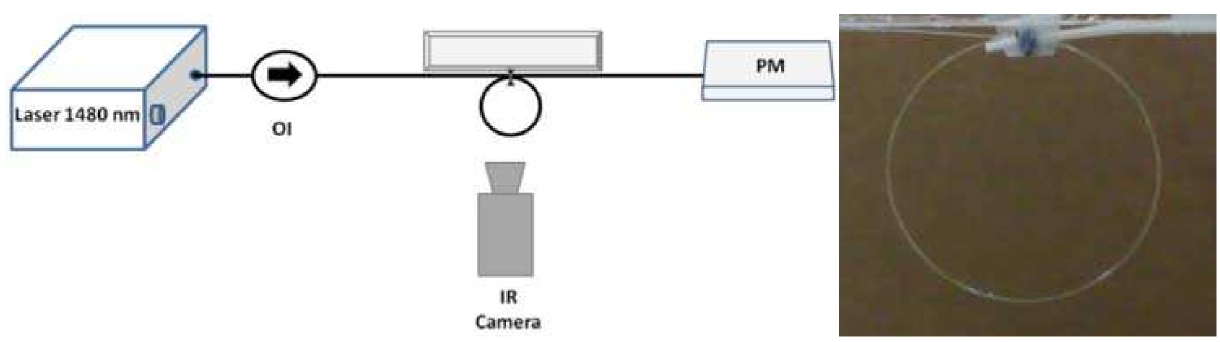

a) b)

Fig. 11. a) Diagram of the experimental setup, and b) photograph of the circular loop with a diameter of 12.50mm

The temperature in the bent region was measured with an infrared thermal camera (ThermaCAM™ Flir i40). The optical signal source was a Raman laser (IPG - RLR-10-1480), emitting at the wavelength of 1480 nm, with a maximum optical power of 2W. To determine

the total attenuation in the curved section of the fiber, the optical signal output was analyzed with an optical power meter (EXFO FPM-600).
The most common type of fiber used in optical networks is the SMF28.G652.D, thus this fiber was the one studied on the work presented here. The fiber, produced by Corning, has an outer diameter of 125 µm, a core diameter of 10 µm and a primary acrylate coating with an external diameter of 250 µm. The environmental temperature at which the tests took place was 23ºC.
Examples of thermal images captured during the experiments are presented in Fig. 12. These two images were taken for two different bend diameters, after one minute of exposure to high optical powers (1.75 W). It is perceptible that the temperature in the curved section is rising considerably with the decrease of the bend diameter.

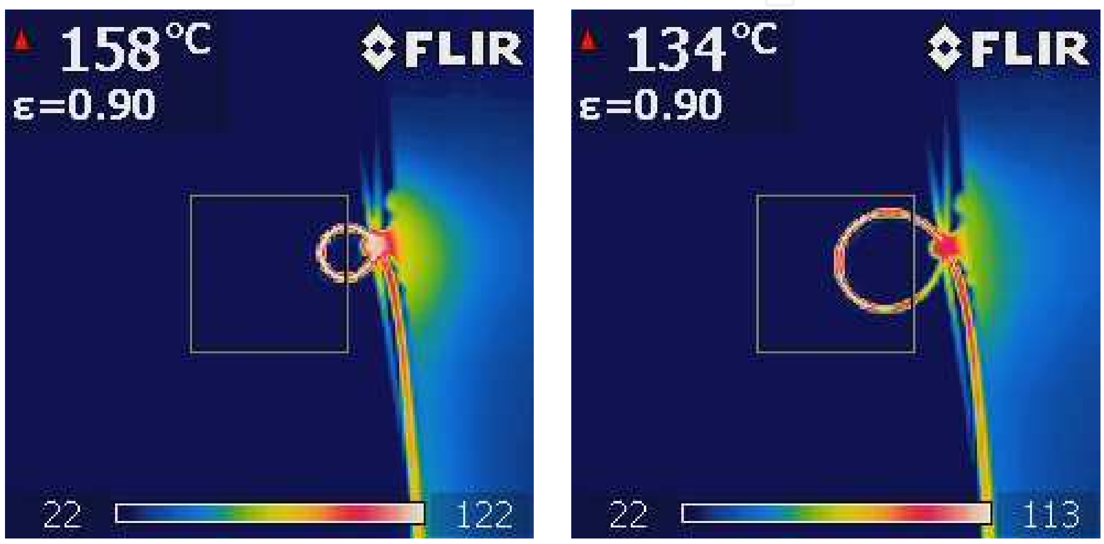

a) b)

Fig. 12. Thermal image of the fiber bending section for an injected optical power of 1.75W and bending diameters of a) 4.86 mm and b) 9.95 mm

Through the analysis of the thermal images, it is evident that, after an initial increase, the temperature stabilizes with time. In Fig. 13, the fiber temperature values obtained for several bending diameters are represented as a function of time. The input optical power was 0.5W for this test.
Considering the above results, all the subsequent measures were made in the stationary regime, i.e., 60 s after the optical power has been turned on. The critical bend diameter is 20 mm, since for higher diameters the rise of the injected optical power as no significant impact in the temperature increase (Andre et al., 2009).
Fig. 14 shows the maximum temperature increase values as function of the injected optical power for different bending diameters.
The observed behavior confirms the relation previously described, between the maximum temperature value obtained and the fiber bend diameter (Andre et al., 2010[b;] Andre et al., 2010[c]).
After the exposure to high optical powers, the physical condition of the fiber bent section was observed using an optical microscope (Olympus SZH-ILLD). Fig. 15 displays two obtained images, showing a fiber that has been submitted to an optical power of 1.5W, and a bend diameter of 2.9 mm during 60 s.

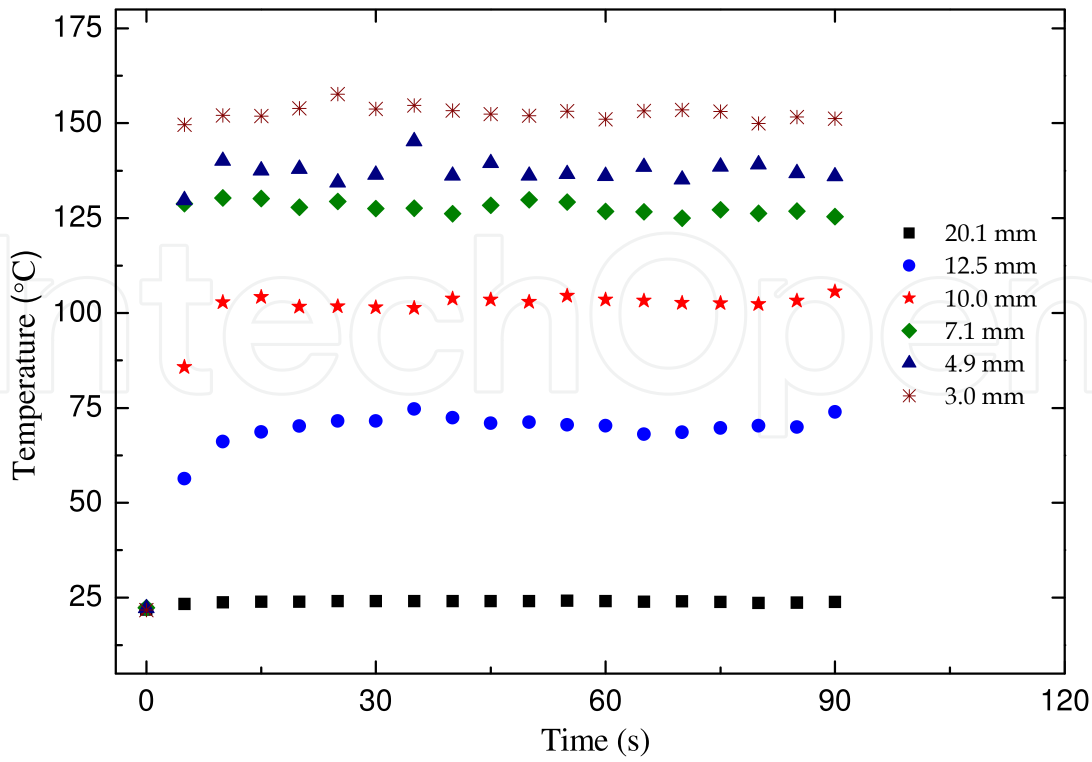

Fig. 13. Temperature values in the bent region along time

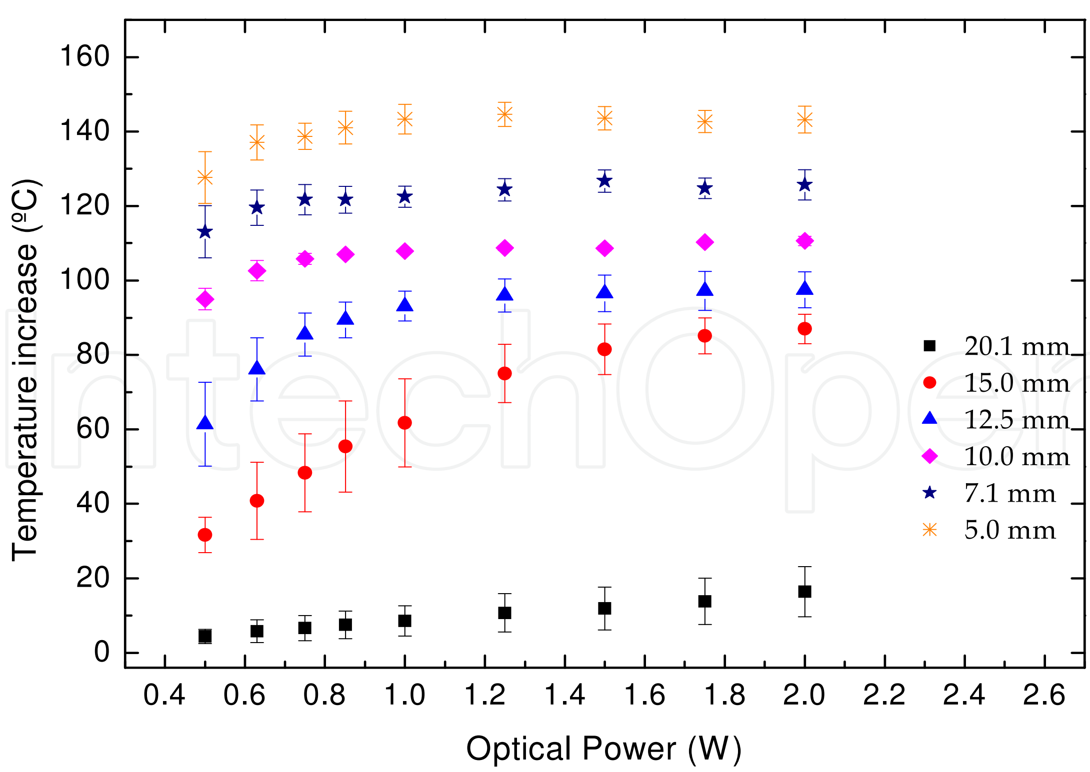

Fig. 14. Maximum temperature increase achieved as function of the optical power injected for several values of bending diameters

Fig. 15. Image of the fiber bend section, after being submitted to an optical power of 1.5W. The bending diameter was 2.9mm and the exposure time was 60 s (magnification of X5)

There, the damage induced by the optical power on the fiber coating in the bent section is well visible. There is degradation of the acrylate and its physical detachment from the silica.

4.1 Modelling the fibre temperature

The damage in the fiber coating is inflicted by the optical power loss in the bent section , which induces the temperature increase of the coating, resulting in an oxidation of the acrylate layer. The optical power irradiated from the optical fiber core is given by:

$$\Delta P = P_{in}\left(1 - 10\left(-\frac{\alpha_{fiber} L}{10}\right)\right) \quad (3)$$

where P_{in} is the optical power injected in the fiber, α_{fiber} is the power loss associated to the bend, expressed in dB/m and L is the length of bent fiber section.

The relation between the temperature increase and the power loss in the bent region is presented in Fig. 16. This graph shows that, independently of the bending diameter, the maximum temperature changes nonlinearly with the optical power loss, showing some stabilization for optical power losses around 0.3 W (Andre et al., 2010[b]). The differences observed in the maximum temperature for the several bending diameter can be explained by the fact that some of the energy that is lost from the core guided mode can be guided in the cladding (Andre et al., 2010[b]).

Assuming a thermal model that considers that the optical signal energy transferred to non guided modes is absorbed by the acrylate layer and then converted into heat, it is possible to estimate the temperature in the bent region. Nevertheless, due to the absorption saturation of the coating observed for higher optical powers not all the energy is absorbed (Andre et al., 2010[b]). In the stationary regime, the heat source (P_{in}) given by the radiation absorbed in the acrylate is converted in stored heat in the fiber (Q_{stored}) and in heat loss to the exterior (Q_{out}), which can be modeled considering a heat transfer coefficient (h) (Andre et al., 2010[b]).

$$Q_{stored} = \rho c_p A l \frac{dT}{dt} \quad (4)$$

$$Q_{out} = \pi d l h (T - T_0) \quad (5)$$

where d and l are the diameter and length of the fiber bent section, respectively. T_0 is the environment temperature, A is the optical fiber area and ρ and c_p are the density and specific heat of the fiber (considering an average value for the silica and acrylate), respectively (Andre et al., 2010[b])

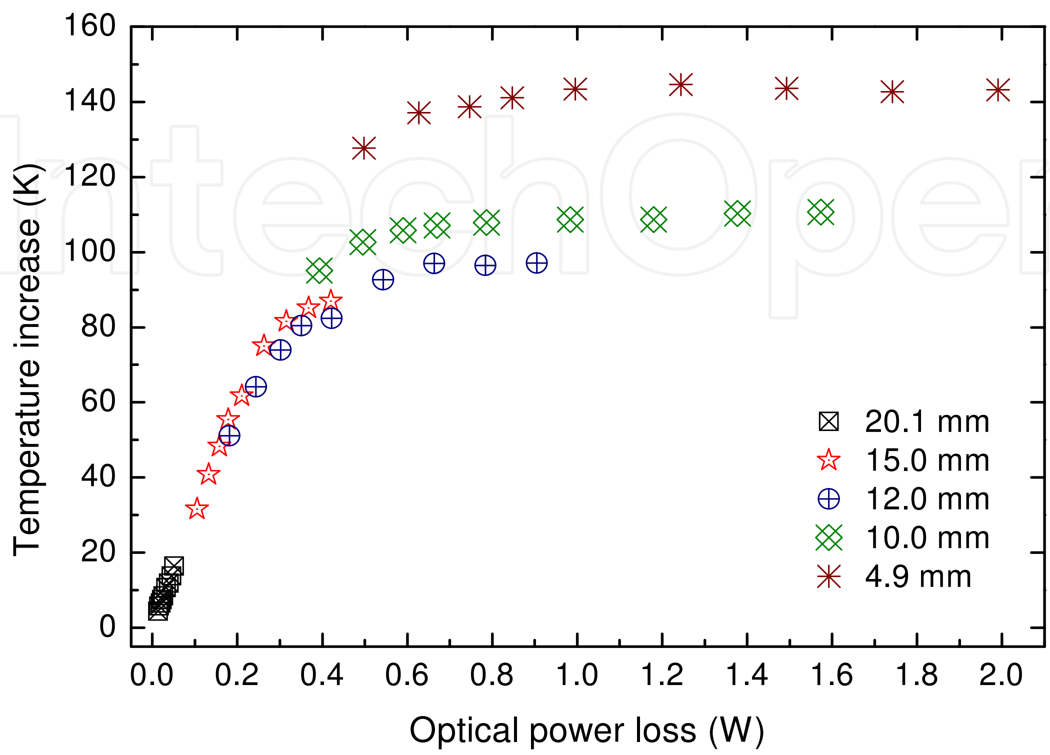

Fig. 16. Temperature as function of the optical power loss for different bending diameters for a propagation signal at 1480 nm

As stated before, in the presence of high optical powers, the absorption in the acrylate layer exhibits a non-linear behavior and thus the power absorbed by the acrylate saturates in a maximum value given by:

$$P_{in} = P_{\max}\left(1-\exp\left(-\beta\Delta P\right)\right) \tag{6}$$

So, in equilibrium, the maximum temperature rise can be expressed as (Andre et al., 2010[b]):

$$\Delta T = \frac{P_{\max}\left(1-\exp\left(-\beta\Delta P\right)\right)}{\pi d l h} \tag{7}$$

Where ΔT is the maximum temperature increase relatively to the environment equilibrium temperature, P_{max} is the maximum optical power absorbed by the coating and β is the activation constant (Andre et al., 2010[b]). The experimental results referred above for maximum temperature increase versus injected optical power for different bending diameters were fitted to the theoretical curve given by equation (7). The results are presented in Fig. 17. The parameters for this theoretical fit were P_{max}/h and β and the reduced chi-square value obtained was of 0.4542.
These results show that is possible to correlate the bend diameter, the injected optical power and the temperature increase in the optical fiber coating. This model can be useful for the design of future systems, being an approach to limit the bending diameter to values that

depend on the injected power, in order to maintain the operational conditions below a safety limit.

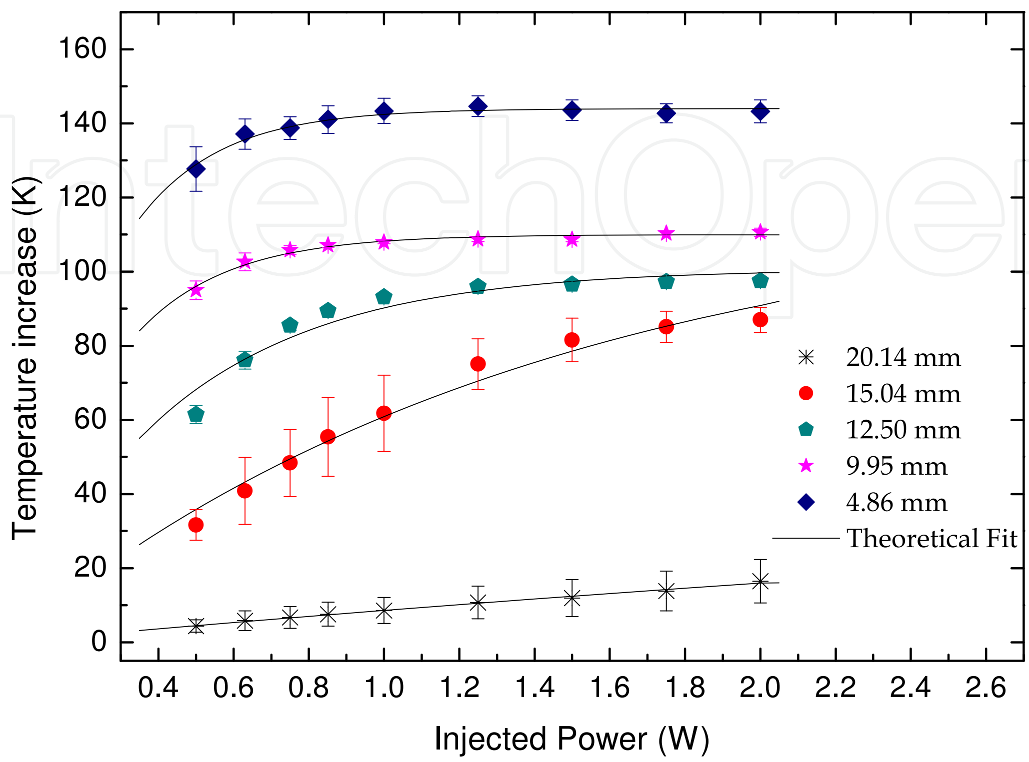

Fig. 17. Optical fiber maximum temperature increase as function of injected optical power for different values of bending diameter. Dots are experimental results and the lines are the fitting results, with $P_{max}/h=0.00245\pm0.00010$ K·m^2 and $\beta=5.03\pm0.68$ W^{-1}

5. Conclusions

In this work, we have analyzed the thermal effects occurring in an optical fiber. We have shown that the maximum power required to extinguish the optical discharge propagation is 1.39 W. It was also shown that the critical bending diameter for SMF fibers with high power signal is 20 mm.
These results describe the main thermal affects occurring in an optical fibre used in telecommunications.

6. References

Abedin, K. S. and T. Morioka (2009). Remote Detection of Fiber Fuse Propagating in Optical Fibers, *Proceedings of Conference on Optical Fiber Communication, collocated National Fiber Optic Engineers Conference* Vol. 1-5, pp. OThD5, San Diego, CA, USA.

Andre, P. S., M. Facao, A. M. Rocha, P. Antunes and A. Martins (2010[a]). Evaluation of the fuse effect propagation in networks infrastructures with different types of fibers, *Proceedings of Conference on Optical Fiber Communication, collocated National Fiber Optic Engineers Conference* pp. JWA10, San Diego, CA, USA.

Andre, P. S., A. M. Rocha, F. Domingues and A. Martins (2010[b]). Improved thermal model for optical fibre coating owing to small bending diameter and high power signals, *Electronics Letters*, Vol. 46, No. 10, pp. 695-696, ISSN: 0013-5194.

Andre, P. S., A. M. Rocha, F. Domingues and A. Martins (2010[c]). Thermal model for optical fiber coating under tight bending diameters, *Proceedings of 15th OptoeElectronics and Communications Conference* pp. 318-319, Sapporo, Japan.

Andre, P. S., A. M. Rocha, B. Neto, A. Martins, M. Facao, J. L. Pinto, A. L. J. Teixeira, R. N. Nogueira, M. J. Lima, G. Incerti, D. Forin and G. T. Beleffi (2009). Optical Fiber Bending Limits for Optical Fiber Infraestructures, *Proceedings of IEEE Africon*, pp. 882-884, Nairobi, Kenya.

Atkins, R. M., P. G. Simpkins and A. D. Yablon (2003). Track of a fiber fuse: a Rayleigh instability in optical waveguides, *Optics Letters*, Vol. 28, No. 12, pp. 974-976, ISSN: 0146-9592.

Bigot-Astruc, M., L. A. de Montmorillon and P. Sillard (2008). High-Power Resistance of Bend-Optimized Single-Mode Fibers, *Proceedings of Conference on Optical Fiber communication / National Fiber Optic Engineers Conference*, pp. JWA2, San Diego, CA, USA.

Bigot-Astruc, M., P. Sillard, S. Gauchard, P. Le Roux and E. Brandon (2006). Analysis of coating temperature increase in fibers under high power and tight bending, *Proceedings of Optical Fiber Communication Conference/National Fiber Optic Engineers Conference*, pp. OFK4, Anaheim, CA, USA.

Davis, D. D., S. C. Mettler and D. J. DiGiovanni (1997). A comparative evaluation of fiber fuse models, *Proceedings of SPIE*, Vol. 2966, pp. 592-606.

Davis, I. M., G. S. Glaesemann, S. Ten and M. J. Winningham (2005). Optical fibres resilient to failure in bending under high power, *Proceedings of 31st European Conference on Optical Communication*, Vol. 3, pp. We3.4.5, ISBN 0537-9989.

Dianov, E. M., I. A. Bufetov and A. A. Frolov (2004[a]). Destruction of silica fiber cladding by the fuse effect, *Optics Letters*, Vol. 29, No. 16, pp. 1852-1854, ISSN: 0146-9592.

Dianov, E. M., I. A. Bufetov, A. A. Frolov, Y. K. Chamorovsky, G. A. Ivanov and I. L. Vorobjev (2004[b]). Fiber fuse effect in microstructured fibers, *Ieee Photonics Technology Letters*, Vol. 16, No. 1, pp. 180-181, ISSN: 1041-1135.

Dianov, E. M., V. E. Fortov, I. A. Bufetov, V. P. Efremov, A. E. Rakitin, M. A. Melkumov, M. I. Kulish and A. A. Frolov (2006). High-speed photography, spectra, and temperature of optical discharge in silica-based fibers, *Ieee Photonics Technology Letters*, Vol. 18, No. 5-8, pp. 752-754, ISSN: 1041-1135.

Driscoll, T. J., J. M. Calo and N. M. Lawandy (1991). Explaining the Optical Fuse, *Optics Letters*, Vol. 16, No. 13, pp. 1046-1048, ISSN: 0146-9592.

Facao, M., A. M. Rocha and P. S. Andre (2011). Traveling Solutions of the Fuse Effect in Optical Fibers, *Journal of Lightwave Technology*, Vol. 29, No. 1, pp. 109-114, ISSN: 0733-8724.

Giraldi, M. T. M. R., A. M. Rocha, B. Neto, C. Correia, M. E. V. Segatto, M. J. Pontes, A. P. L. Barbero, J. C. W. Costa, M. A. G. Martinez, O. Frazao, J. M. Baptista, H. M. Salgado, M. B. Marques, A. L. J. Teixeira and P. S. Andre (2009). Brillouin Effects in Distributed Raman Amplifiers under Saturated Conditions, *Proceedings of Ieee Mtt-S International Microwave and Optoelectronics Conference* pp. 831-835

Glaesemann, G. S., M. J. Winningham, D. A. Clark, J. Coon, S. E. DeMartino, S. L. Logunov and C. K. Chien (2006). Mechanical failure of bent optical fiber subjected to high power, *Journal of the American Ceramic Society*, Vol. 89, No. 1, pp. 50-56, ISSN: 0002-7820.

Hanafusa, H., Y. Hibino and F. Yamamoto (1985). Formation Mechanism of Drawing-Induced E' Centers in Silica Optical Fibers, *Journal of Applied Physics*, Vol. 58, No. 3, pp. 1356-1361, ISSN: 0021-8979.

Hand, D. P. and T. A. Birks (1989). Single-Mode Tapers as Fiber Fuse Damage Circuit-Breakers, *Electronics Letters*, Vol. 25, No. 1, pp. 33-34, ISSN: 0013-5194.

Hand, D. P. and P. S. Russell (1988[a]). Solitary thermal shock waves and optical damage in optical fibers: the fiber fuse, *Optics Letters*, Vol. 13, No. 9, pp. 767-769, ISSN: 0146-9592

Hand, D. P. and P. S. J. Russell (1988[b]). Soliton-like thermal shock-waves in optical fibres: origin of periodic damage tracks, *Proceedings of Fourteenth European Conference on Optical Communication*, pp. 111-114 vol.111.

Hanzawa, N., K. Kurokawa, K. Tsujikawa, K. Takenaga, S. Tanigawa, S. Matsuo and S. Tomita (2010). Observation of a propagation mode of a fiber fuse with a long-period damage track in hole-assisted fiber, *Optics Letters*, Vol. 35, No. 12, pp. 2004-2006, ISSN: 0146-9592.

Harris, A. J. and P. F. Castle (1986). Bend Loss Measurements on High Numerical Aperture Single-Mode Fibers as a Function of Wavelength and Bend Radius, *Journal of Lightwave Technology*, Vol. 4, No. 1, pp. 34-40, ISSN: 0733-8724.

Kashyap, R. (1987). Self-propelled self-focusing damage in optical fibers, *Proceedings of X International Conference on Lasers*, Lake Tahoe.

Kashyap, R. and K. J. Blow (1988). Observation of Catastrophic Self-Propelled Self-Focusing in Optical Fibers, *Electronics Letters*, Vol. 24, No. 1, pp. 47-49, ISSN: 0013-5194.

Kashyap, R., A. H. Sayles and G. F. Cornwell (1997). Heat-flow modeling and visualization of catastrophic self-propagating damage in single-mode optical fibers at low powers, *Proceedings of SPIE*, Vol. 2966, pp. 586-591.

Lee, M. M., J. M. Roth, T. G. Ulmer and C. V. Cryan (2006). The fiber fuse phenomenon in polarization-maintaining fibers at 1.55 μm, *Proceedings of Lasers and Electro-Optics and Quantum Electronics and Laser Science Conference*, pp. JWB66, Long Beach, CA, USA.

Logunov, S. L. and M. E. DeRosa (2003). Effect of coating heating by high power in optical fibres at small bend diameters, *Electronics Letters*, Vol. 39, No. 12, pp. 897-898, ISSN: 0013-5194.

Marcuse, D. (1976). Curvature Loss Formula for Optical Fibers, *Journal of the Optical Society of America*, Vol. 66, No. 3, pp. 216-220, ISSN: 0030-3941.

Martins, A., A. M. Rocha and P. S. Andre (2009). High power effects on fiber optic connectors, *Proceedings of International Microwave and Optoelectronics Conference (IMOC)*, ISBN 1679-4389, Belem, Brazil.

Percival, R. M., E. S. R. Sikora and R. Wyatt (2000). Catastrophic damage and accelerated ageing in bent fibres caused by high optical powers, *Electronics Letters*, Vol. 36, No. 5, pp. 414-416, ISSN: 0013-5194.

Rocha, A. M., P. Antunes, F. Domingues, M. Facao and P. S. Andre (2011) Detection of Fiber Fuse Effect Using FBG Sensors. *IEEE Sensors Journal,* DOI: 10.1109/JSEN.2010.2094183

Rocha, A. M., M. Facão and P. S. André (2010). Study of fiber fuse effect on different types of single mode optical fibers, *Proceedings of Network and Optical Communications*, pp. 75-79, Faro, Portugal.

Rocha, A. M., A. Martins, M. Facao and P. S. Andre (2009[a]). Effect of bending in SMF fibers under high power, *Proceedings of 11th International Conference on Transparent Optical Networks*, pp. Th.B2.1, Azores, Portugal.

Rocha, A. M., B. Neto, A. Martins, G. Incerti, D. Forin, G. Bellefi, M. Facao, J. L. Pinto, A. L. J. Teixeira, R. N. Nogueira, M. J. Lima and P. S. Andre (2009[b]). The effect of high power propagation in bended fibers, *Proceedings of 10th International Conference onTelecommunications.* , pp. 303-304.

Schermer, R. T. and J. H. Cole (2007). Improved bend loss formula verified for optical fiber by simulation and experiment, *Ieee Journal of Quantum Electronics*, Vol. 43, No. 9-10, pp. 899-909, ISSN: 0018-9197.

Seo, K., N. Nishimura, M. Shiino, R. Yuguchi and H. Sasaki (2003). Evaluation of High-power Endurance in Optical Fiber Links, *Furukawa Review*, Vol. 24, pp. 17-22,

Sergeev, O. A., A. G. Shashkov and A. S. Umanskii (1982). Thermophysical properties of quartz glass, *Journal of Engineering Physics and Thermophysics*, Vol. 43, No. 6, pp. 1375-1383, ISSN: 1062-0125.

Shuto, Y. (2010). Evaluation of High-Temperature Absorption Coefficients of Ionized Gas Plasmas in Optical Fibers, *Ieee Photonics Technology Letters*, Vol. 22, No. 3, pp. 134-136, ISSN: 1041-1135.

Shuto, Y., S. Yanagi, S. Asakawa, M. Kobayashi and R. Nagase (2004[a]). Fiber fuse phenomenon in step-index single-mode optical fibers, *Ieee Journal of Quantum Electronics*, Vol. 40, No. 8, pp. 1113-1121, ISSN: 0018-9197.

Shuto, Y., S. Yanagi, S. Asakawa, M. Kobayashi and R. Nagase (2004[b]). Evaluation of high-temperature absorption coefficients of optical fibers, *Ieee Photonics Technology Letters*, Vol. 16, No. 4, pp. 1008-1010, ISSN: 1041-1135.

Shuto, Y., S. Yanagi, S. Asakawa, M. Kobayashi and R. Nagase (2004[c]). Fiber fuse generation in single-mode fiber-optic connectors, *Ieee Photonics Technology Letters*, Vol. 16, No. 1, pp. 174-176, ISSN: 1041-1135.

Shuto, Y., S. Yanagi, S. Asakawa and R. Nagase (2003). Generation mechanism on fiber fuse phenomenon in single-mode optical fibers, *Electronics and Communications in Japan Part Ii-Electronics*, Vol. 86, No. 11, pp. 11-20, ISSN: 8756-663X.

Sikora, E. S. R., D. J. McCartney and J. V. Wright (2007). Impact of coating ageing on susceptibility to high-power damage at fibre bends, *Electronics Letters*, Vol. 43, No. 4, pp. 208-210, ISSN: 0013-5194.

Todoroki, S. (2005[a]). In-situ observation of fiber-fuse propagation, *Japanese Journal of Applied Physics Part 1-Regular Papers Short Notes & Review Papers*, Vol. 44, No. 6A, pp. 4022-4024, ISSN: 0021-4922.

Todoroki, S. (2005[b]). Origin of periodic void formation during fiber fuse, *Optics Express*, Vol. 13, No. 17, pp. 6381-6389, ISSN: 1094-4087.

Todoroki, S. (2005[c]). Animation of fiber fuse damage, demonstrating periodic void formation, *Optics Letters*, Vol. 30, No. 19, pp. 2551-2553, ISSN: 0146-9592.

Todoroki, S. (2005[d]). Transient propagation mode of fiber fuse leaving no voids, *Optics Express*, Vol. 13, No. 23, pp. 9248-9256, ISSN: 1094-4087.

Valiente, I. and C. Vassallo (1989). New Formalism for Bending Losses in Coated Single-Mode Optical Fibers, *Electronics Letters*, Vol. 25, No. 22, pp. 1544-1545, ISSN: 0013-5194.

Wang, J., S. Gray, D. Walton and L. Zantano (2008). Fiber Fuse in High power optical fiber, *Proceedings of SPIE*, Vol. 7134, pp. 2E-1-9.

Yakovlenko, S. I. (2006[a]). Mechanism for the void formation in the bright spot of a fiber fuse, *Laser Physics*, Vol. 16, No. 3, pp. 474-476, ISSN: 1054-660X.

Yakovlenko, S. I. (2006[b]). Physical processes upon the optical discharge propagation in optical fiber, *Laser Physics*, Vol. 16, No. 9, pp. 1273-1290, ISSN: 1054-660X.

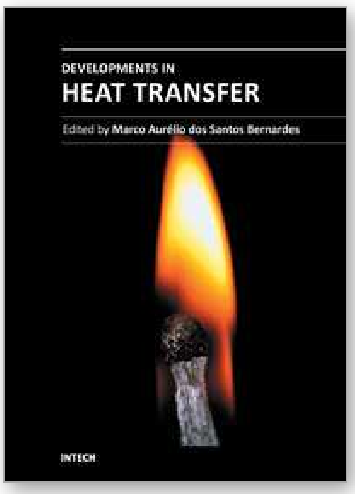

Developments in Heat Transfer

Edited by Dr. Marco Aurelio Dos Santos Bernardes

ISBN 978-953-307-569-3
Hard cover, 688 pages
Publisher InTech
Published online 15, September, 2011
Published in print edition September, 2011

This book comprises heat transfer fundamental concepts and modes (specifically conduction, convection and radiation), bioheat, entransy theory development, micro heat transfer, high temperature applications, turbulent shear flows, mass transfer, heat pipes, design optimization, medical therapies, fiber-optics, heat transfer in surfactant solutions, landmine detection, heat exchangers, radiant floor, packed bed thermal storage systems, inverse space marching method, heat transfer in short slot ducts, freezing an drying mechanisms, variable property effects in heat transfer, heat transfer in electronics and process industries, fission-track thermochronology, combustion, heat transfer in liquid metal flows, human comfort in underground mining, heat transfer on electrical discharge machining and mixing convection. The experimental and theoretical investigations, assessment and enhancement techniques illustrated here aspire to be useful for many researchers, scientists, engineers and graduate students.

INTECH
open science | open minds

InTech Europe
University Campus STeP Ri
Slavka Krautzeka 83/A
51000 Rijeka, Croatia
Phone: +385 (51) 770 447
Fax: +385 (51) 686 166
www.intechopen.com

InTech China
Unit 405, Office Block, Hotel Equatorial Shanghai
No.65, Yan An Road (West), Shanghai, 200040, China
中国上海市延安西路65号上海国际贵都大饭店办公楼405单元
Phone: +86-21-62489820
Fax: +86-21-62489821